Supplementary Information

Structural phase transitions of $(Bi_{1-x}Sb_x)_2(Te_{1-y}Se_y)_3$ compounds under high pressure and the influence of the atomic radius on the compression processes of tetradymites†

Jinggeng Zhao,*‡[ab] Zhenhai Yu,‡[c] Qingyang Hu,[cd] Yong Wang,[a] John Schneeloch,[e] Chunyu Li,[c] Ruidan Zhong,[e] Yi Wang,[ab] Zhiguo Liu*[a] and Genda Gu[e]

[a]*Department of Physics, Harbin Institute of Technology, Harbin 150080, China, E-mail: liuzhiguo@hit.edu.cn*

[b]*Natural Science Research Center, Academy of Fundamental and Interdisciplinary Sciences, Harbin Institute of Technology, Harbin 150080, China, E-mail: zhaojinggeng@163.com*

[c]*Center for High Pressure Science and Technology Advanced Research, Shanghai 201203, China*

[d]*Department of Geological Sciences, Stanford University, Stanford, CA 94305, USA*

[e]*Condensed Matter Physics and Materials Science Department, Brookhaven National Laboratory, Upton, NY 11973, USA*

†Electronic Supplementary Information (ESI): Schematic views of the crystal structures of A_2B_3-type tellurides and selenides (Fig. S1), experimental lattice parameters and atomic coordinates of phase IV of Bi_2Te_2Se (Table S1), calculated lattice parameters and atomic coordinates of Bi_2Te_2Se (Table S2), XRD patterns of $BiSbTeSe_2$ and Sb_2Te_2Se under high pressure (Fig. S2), fitted results of equation of state for A_2B_3-type tellurides and selenides (Table S3), schematic views of the crystal structures of (a) tetradymite and rock salt and (b) CsCl-like structure units in the BCT and CN9M models (Fig. S3), and progression of one quintuple layer in the tetradymite series (Fig. S4).

‡These authors contributed equally to this study and share first authorship.

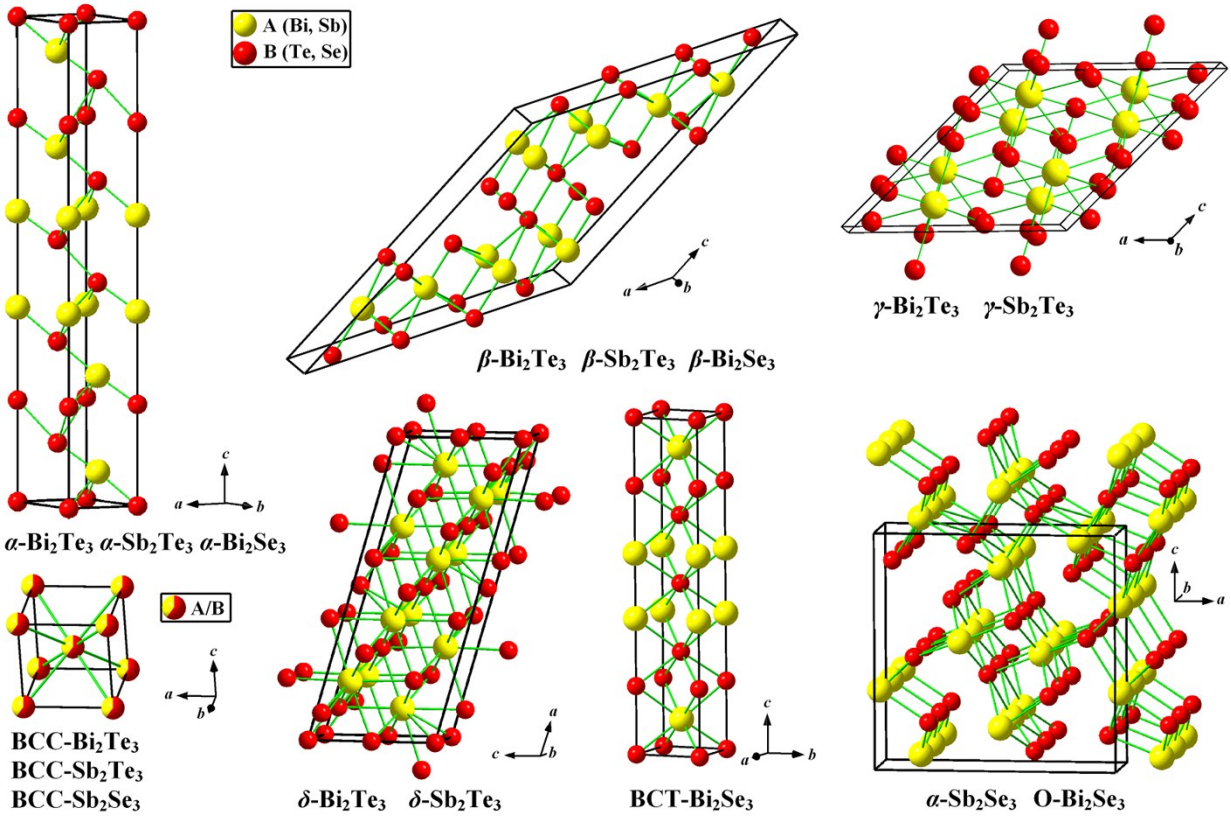

Fig. S1 Schematic views of the crystal structures of A_2B_3-type compounds (A = Bi, Sb; B = Te, Se) at ambient and high pressures. The black bold lines denote the unit cells. For Bi_2Te_3, Sb_2Te_3, and Bi_2Se_3, phase α adopts a hexagonal unit cell and phase β adopts the unit cell from Ref. 5.

Table S1. Lattice parameters and atomic coordinates of phase IV of Bi_2Te_2Se at 30.9 GPa, which are simulated by using the body-centered tetragonal (BCT), 9/10-fold monoclinic (CN9M), and disordered body-centered cubic (BCC) structures

Atom	**Site**	***x***	***y***	***z***
Phase IV (BCT) Space group: *I*4/*mmm*; a = 3.5319(2) Å, c = 17.4573(17) Å; R_p = 1.41%, R_{wp} = 1.69%.				
Bi	4e	0	0	0.4003(2)
Te	4e	0	0	0.2030(2)
Se	2a	0	0	0
Phase IV (CN9M) Space group: *C*2/*m*; a = 15.036(2) Å, b = 4.9914(3) Å, c = 6.0788(4) Å, β = 105.30(1)°; R_p = 2.02%, R_{wp} = 2.96%.				
Bi(1)	4i	0.3992(4)	0	0.6083(8)
Bi(2)	4i	0.1979(6)	0	0.8004(9)
Te(1)	4i	0.8001(6)	0	0.6983(10)
Te(2)	2c	0	0	0.5
Te(3)	2a	0	0	0
Se	4i	0.3992(5)	0	0.0952(11)
Phase IV (disordered BCC) Space group: *Im*-3*m*; a = 3.5192(2) Å; R_p = 3.21%, R_{wp} = 4.80%.				
Bi/Te/Se	2a	0	0	0

Table S2. Calculated lattice parameters and atomic coordinates of Bi_2Te_2Se

Atom	**Site**	***x***	***y***	***z***
Phase I @ 5 GPa (CN6R) * Space group: *R*-3*m*; *a* = 4.2318 Å, *c* = 29.092 Å.				
Bi	6c	0	0	0.3956
Te	6c	0	0	0.2097
Se	3a	0	0	0
Phase II @ 15 GPa (CN7M) ** Space group: *C*2/*m*; *a* = 14.476 Å, *b* = 3.9375 Å, *c* = 8.9271 Å, *β* = 90.55°.				
Bi(1)	4i	0.9749	0	0.1828
Bi(2)	4i	0.2201	0	0.2045
Te(1)	4i	0.8249	0	0.3927
Te(2)	4i	0.4283	0	0.6242
Se	4i	0.3655	0	0.0033
Phase III @ 15 GPa (CN8M) Space group: *C*2/*c*; *a* = 9.7931 Å, *b* = 7.0632 Å, *c* = 10.241 Å, *β* = 135.53°.				
Bi	8f	0.2875	0.1080	0.3525
Te	8f	0.5997	0.3654	0.4625
Se	4e	0	0.3649	0.25
Phase IV @ 30 GPa (BCT) Space group: *I*4/*mmm*; *a* = 3.5345 Å, *c* = 17.1355 Å.				
Bi	4e	0	0	0.4059
Te	4e	0	0	0.1984
Se	2a	0	0	0
Phase IV @ 30 GPa (CN9M) Space group: *C*2/*m*; *a* = 14.845 Å, *b* = 4.9757 Å, *c* = 6.0376 Å, *β* = 105.85°.				
Bi(1)	4i	0.4084	0	0.6429
Bi(2)	4i	0.1939	0	0.8125
Te(1)	4i	0.7934	0	0.6880
Te(2)	2c	0	0	0.5
Te(3)	2a	0	0	0
Se	4i	0.3957	0	0.1115

*Phase I adopts a hexagonal unit cell.

**This structure of phase II in Table S2 is equivalent to that in Ref. 5 with same *a*- and *b*-axis and different *c*-axis and *β* angle.

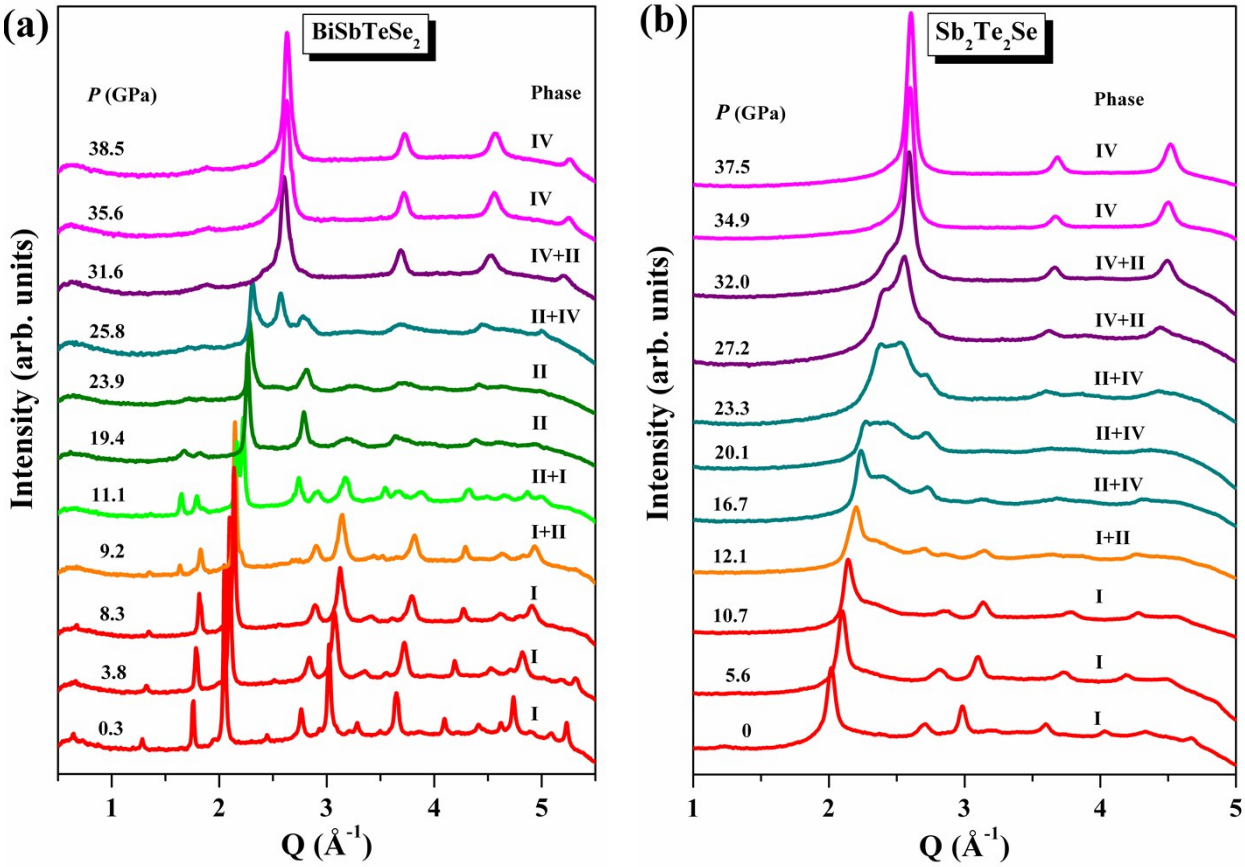

Fig. S2 Selected angle-dispersive X-ray diffraction (AD-XRD) patterns of (a) $BiSbTeSe_2$ and (b) Sb_2Te_2Se at room temperature up to 38.5 and 37.5 GPa, respectively.

Table S3. Bulk modulus (B_0), first-order pressure derivative (B_0), and fitted ambient unit cell volume (V_0/f.u.) of phases I–IV for A_2B_3-type compounds (A = Bi, Sb; B = Te, Se) in this work and references,[7–16,19,20,28,41] in which "NA" and "—" represent no phase and no data, respectively

		Phase I			Phase II			Phase III			Phase IV		
		B_0 (GPa)	B_0	V_0/f.u. (Å^3)	B_0 (GPa)	B_0	V_0/f.u. (Å^3)	B_0 (GPa)	B_0	V_0/f.u. (Å^3)	B_0 (GPa)	B_0	V_0/f.u. (Å^3)
Bi_2Te_2Se	**This work**	49(2)	4	157.2(4)	62(2)	4	149.1(5)	NA	NA	NA	104(4)	4	133.2(7)
	Ref. 41	38.3(17)	5.0	160.6(2)	68(7)	4	129.6(8)	NA	NA	NA	137(5)	4.0	114.9(1)
$Bi_2Te_{1.75}Se_{1.19}$	**Ref. 41**	34.5(10)	6.2	158.92(18)	77(3)	4	127.3(2)	NA	NA	NA	146(3)	4.0	111.42(6)
$BiSbTe_2Se$	**This work**	46.5(7)	4	146.2(2)	55(1)	4	140.0(6)	NA	NA	NA	63(5)	4	130.6(1.8)
Sb_2Te_2Se	**This work**	44(2)	4	151.0(6)	60(4)	4	143.1(1.2)	NA	NA	NA	73(4)	4	133.1(1.1)
Bi_2Te_3	**Ref. 7**	21.85(20)	17.13 (<2.0 GPa)		—	—	—	—	—	—	—	—	—
		38.19(42)	4.61 (>2.0 GPa)		—	—	—	—	—	—	—	—	—
	Ref. 8	41.92 (Calc.)	4.89	—	41.25 (Calc.)	4.06	—	45.28 (Calc.)	3.57	—	—	—	—
		41.61 (Calc.)	4.68	—	—	—	—	—	—	—	—	—	—
	Ref. 9	28.1(1.0)	13.8 (<3.2 GPa)		—	—	—	—	—	—	—	—	—
		36.3(1.0)	5.5 (>3.2 GPa)		—	—	—	—	—	—	—	—	—
	Ref. 10	56.2(12)	2.1	169.16(7)	112(6)	6	148.3(7)	—	—	—	—	—	—
$BiSbTe_3$	**Ref. 10**	56(2)	5.27	164.7(2)	97.5(27)	6.15	147.2(3)	—	—	—	—	—	—
Sb_2Te_3	**Ref. 11**	54.7(2)	4	157.5(1)	77.1(5)	4	148.5(8)	80.5(6)	4	140.0(6)	109.4(4)	4	127.5(5)
	Ref. 12	45(2)	4	158.4(5)	62(3)	4	148.7(8)	69(4)	4	143(1)	72(2)	4	136.5(7)
	Ref. 13	41.0 (Calc.)	5.2	158.1	34.74 (Calc.)	5	—	38.91 (Calc.)	5	—	—	—	—
	Ref. 14	36.1(9)	6.2	—	—	—	—	—	—	—	—	—	—
	Ref. 15	40	4.0	158.3	—	—	—	—	—	—	—	—	—
	Ref. 10	30.2(14)	9.4	159.7(2)	60.8(26)	3.4	146.8(5)	—	—	—	—	—	—
Bi_2Se_3	**Ref. 16**	53.1(7)	4	141.2(2)	66(2)	4	133.4(6)	NA	NA	NA	97(3)	4	123.3(6)
	Ref. 19	53(8) (Exp.)	2.9	—	66(3) (Exp.)	4.5	—	—	—	—	—	—	—
		47.8 (Calc.)	3.9	—	60.4 (Calc.)	4.8	—	77.1 (Calc.)	2.6	—	—	—	—
		48.0 (Calc.)	4.6	—	—	—	—	—	—	—	—	—	—
	Ref. 20	32.9(8)	5.1	—	—	—	—	—	—	—	—	—	—
Sb_2Se_3	**Ref. 28**	30(1)	6.1	136.4	NA	NA	NA	NA	NA	NA	217(11)	4	87.25(10)

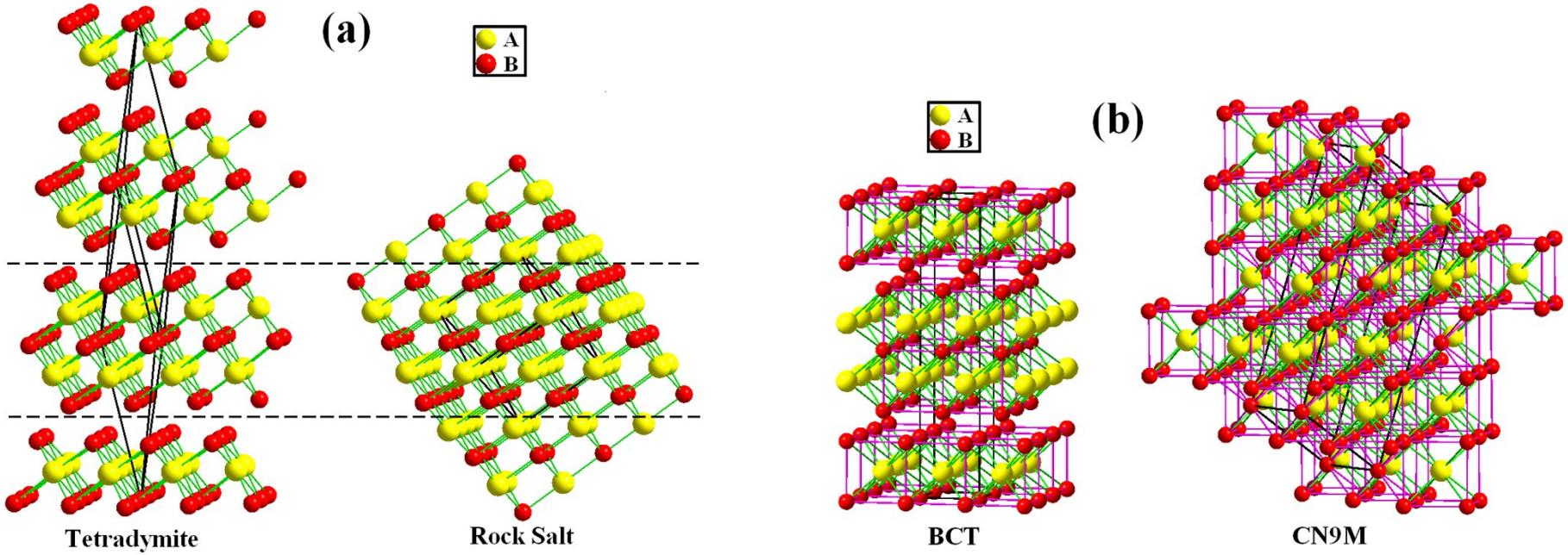

Fig. S3 Schematic views of (a) the crystal structures of tetradymite and rock salt along the body diagonal direction and (b) the CsCl-like structure units in the BCT and CN9M models. The black bold lines denote the unit cells.

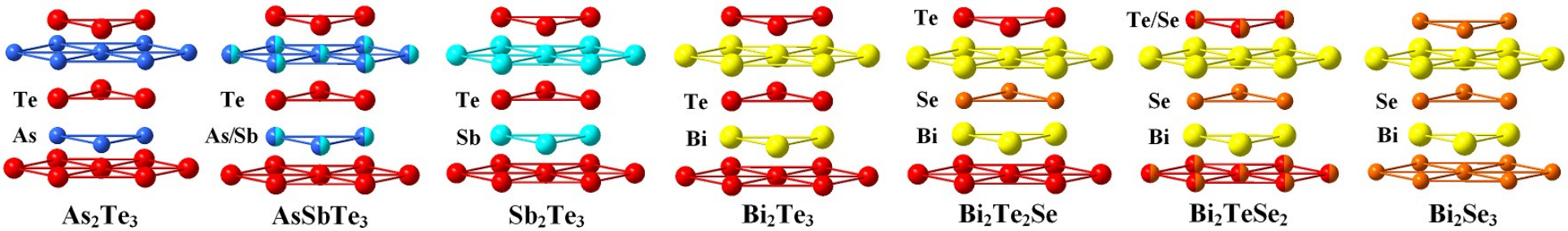

Fig. S4 Progressions of one quintuple layer in the tetradymite series, including As_2Te_3, $AsSbTe_3$, Sb_2Te_3, Bi_2Te_3, Bi_2Te_2Se, Bi_2TeSe_2, and Bi_2Se_3. We have used Cava's work for reference to draw this figure.[79]